International Journal of Geo-Information

MDPI

*Review*

# Analysis and Applications of GlobeLand30: A Review

**Jun Chen [1,*], Xin Cao [2,3], Shu Peng [1] and Huiru Ren [1]**

1 National Geomatics Center of China, Beijing 100830, China; pengshu@nsdi.gov.cn (S.P.); renhr.12b@igsnrr.ac.cn (H.R.)
2 State Key Laboratory of Earth Surface Processes and Resource Ecology, Beijing Normal University, Beijing 100875, China; caoxin@bnu.edu.cn
3 Institute of Remote Sensing Science and Engineering, Faculty of Geographical Science, Beijing Normal University, Beijing 100875, China
* Correspondence: chenjun@nsdi.gov.cn; Tel.: +86-10-6388-1088

Academic Editor: Wolfgang Kainz
Received: 16 May 2017; Accepted: 17 July 2017; Published: 27 July 2017

**Abstract:** GlobeLand30, donated to the United Nations by China in September 2014, is the first wall-to-wall 30 m global land cover (GLC) data product. GlobeLand30 is widely used by scientists and users around the world. This paper provides a review of the analysis and applications of GlobeLand30 based on its data-downloading statistics and published studies. An average accuracy of 80% for full classes or one single class is achieved by third-party researchers from more than 10 countries through sample-based validation or comparison with existing data. GlobeLand30 has users from more than 120 countries on five continents, and from all five Social Benefit Areas. The significance of GlobeLand30 is demonstrated by a number of published papers dealing with land-cover status and change analysis, cause-and-consequence analysis, and the environmental parameterization of Earth system models. Accordingly, scientific data sharing in the field of geosciences and Earth observation is promoted, and fine-resolution GLC mapping and applications worldwide are stimulated. The future development of GlobeLand30, including comprehensive validation, continuous updating, and monitoring of sustainable development goals, is also discussed.

**Keywords:** global land cover; analysis; accuracy; status and change; cause and consequence; sustainable development goals

## 1. Introduction

Land cover refers to the biophysical material over the surface of the Earth and immediate sub-surfaces and man-made structures [1]. In the last three centuries, and particularly the past few decades, humans have extensively modified the Earth's land cover because of continuing population and economic growth. Although these changes enabled the provision of critical material goods or resources (i.e., food, fiber, shelter, and freshwater) for immediate human needs, they have also undermined environmental conditions, ecosystem services, and human welfare in the long run [2–4]. For example, the expansion of cropland or urbanization at the cost of forests results in an increase of atmospheric carbon dioxide or urban heat islands [5]. Moreover, land cover changes have significant impacts on ecosystem structures and functioning, greenhouse gases (GHG) emissions, continental and global atmospheric circulation, nutrient and hydrological cycles, biogeo-chemical cycles, as well as biodiversity [4,5]. Reducing negative impacts of land cover change on our planet while sustaining the production of essential resources has become a major concern and challenge for policy-makers and the scientific community around the world [2,6,7].

Land cover and change information is fundamental for understanding the state, trends, drivers, and impacts of different land activities on social and natural processes, as well as designing

transformations towards sustainable development [8–10]. A number of global land cover (GLC) datasets had been developed and used in environmental change studies, Earth system simulation, sustainable development, and many other areas [11–13]. These applications can be classified into three groups. The first is generic statistical analysis, which derives spatially-referenced and quantitative information from the land cover datasets, including acreage statistics and geographic distribution (i.e., the extent and patterns), magnitude and type of change (i.e., expansion, shrinkage or intensification, actual areas altered) [4,14]. Such studies provide insight into the state, patterns, and changes of the main land cover classes. The second group addresses how the land cover pattern forms, that is, global divergence of artificial surface [15] and local urban expansion patterns [16], as well as how the land cover change affects the environment, such as the evaluation of ecosystem services [17,18], estimates of carbon dioxide evasion [19], impact on the terrestrial water cycle [20], and so on. The third incorporates land cover information into earth system models to simulate the climate, biological, geochemical processes, as well as to forecast future environmental conditions and their consequences [4,6].

Reliable GLC data at higher spatial, temporal, and thematic resolutions is the key to success for many applications. Previous coarse spatial resolution (300 m–1 km) GLC datasets did not provide sufficient spatial and thematic details of land activities, and has limited their usability in both scientific analysis and forecasting, policy debate, and political decisions [21,22]. Given the free availability of Landsat and similar resolution satellite data, a few 30 m GLC datasets had been developed and released in the past few years, including a decadal-scale global forest cover change data [23], and a wall-to-wall GLC data product (GlobeLand30) that shows change in ten land cover types and ten years [24]. These 30 m GLC datasets provide more details of land cover patterns, permit the detection of land cover change at the scale of most human land activities, and enable a better understanding of landscape heterogeneity, as well as increase the performance of modeling and simulations [14,21]. They have stimulated the analysis and application of land cover and change in the past few years.

This paper takes GlobeLand30 as an example to review the state-of-the-art of the analysis and applications of the 30 m GLC datasets and to discuss the future directions. Section 2 provides a brief introduction of GlobeLand30 data product and its accuracy analysis. The user distribution and application fields of GlobeLand30 are analyzed in Section 3. Section 4 presents three different types of applications, including status and change analysis, cause and consequence analysis, and coupling analysis with models. Section 5 discusses the future development and application of GlobeLand30.

## 2. GlobeLand30 and Accuracy Analysis

### *2.1. Data Product*

GlobeLand30 is an open-access 30 m resolution global land cover data product that was developed by the National Geomatics Center of China [25]. It comprises ten land cover types, including water bodies, wetlands, artificial surfaces, cultivated lands, forests, shrublands, grasslands, and barren lands (Figure 1), for the years 2000 and 2010. The codes and definition of the ten classes are listed in Table 1. They were extracted from more than 20,000 Landsat and Chinese HJ-1 satellite images with a pixel-object-knowledge (POK)-based operational mapping approach, and an overall classification accuracy of over 80% was achieved [24,26]. On 22 September, China donated GlobeLand30 to the United Nations (UN) as a contribution towards global sustainable development and combating climate change [27]. The GlobeLand30_2010 products were registered at DOI system as DOI:10.11769/GlobeLand30_2010.db, as well as the Global Land Surface Water and Artificial Surface Covers registered as DOI:10.3974/db.2014.02.01 and DOI:10.3974/db.2014.02.02, respectively.

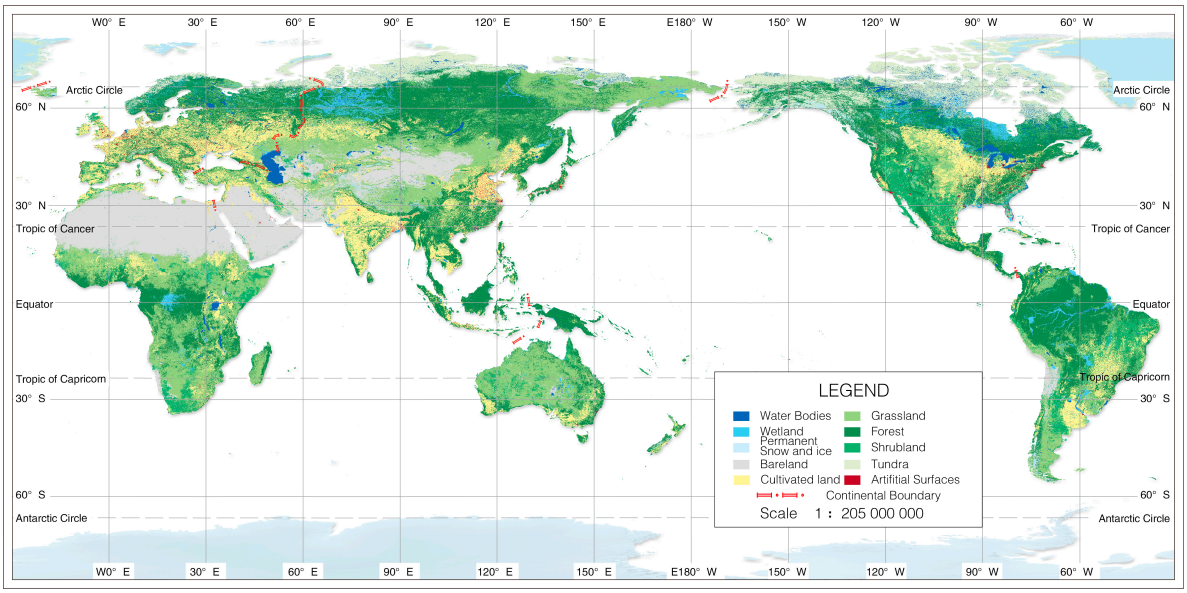


**Figure 1.** Map of GlobeLand30 (2010).

**Table 1.** Classification, codes, and definition of each land cover type of GlobeLand30.

| Code | Type | Definition |
|---|---|---|
| 10 | Cultivated land | Land used for agriculture, horticulture and gardens, including paddy fields, irrigated and dry farmland, vegetable and fruit gardens, etc. |
| 20 | Forest | Land covered by trees, vegetation covers over 30%, including deciduous and coniferous forests, and sparse woodland with cover 10–30%, etc. |
| 30 | Grassland | Land covered by natural grass with cover over 10%, etc. |
| 40 | Shrub land | Land covered by shrubs with cover over 30%, including deciduous and evergreen shrubs, and desert steppe with cover over 10%, etc. |
| 50 | Wetland | Land covered by wetland plants and water bodies, including inland marsh, lake marsh, river floodplain wetland, forest/shrub wetland, peat bogs, mangrove and salt marsh, etc. |
| 60 | Water bodies | Water bodies in land area, including river, lake, reservoir, fish pond, etc. |
| 70 | Tundra | Land covered by lichen, moss, hardy perennial herb and shrubs in the polar regions, including shrub tundra, herbaceous tundra, wet tundra, and barren tundra, etc. |
| 80 | Artificial Surfaces | Land modified by human activities, including all kinds of habitation, industrial and mining area, transportation facilities, and interior urban green zones and water bodies, etc. |
| 90 | Bare land | Land with vegetation cover lower than 10%, including desert, sandy fields, Gobi, bare rocks, saline and alkaline land, etc. |
| 100 | Permanent snow and ice | Lands covered by permanent snow, glacier and icecap. |

GlobeLand30 data adopts raster data format for storage, with the non-destructive GeoTIFF compression format and the 256-color 8-bit indexed pattern. The WGS84 coordinate system, UTM projection and six-degree zoning are adopted. GlobeLand30 is organized into data tiles following two different latitude situations, that is, a size of 5° (latitude) × 6° (longitude) within the area of 60° N and 60° S, and a size of 5° (latitude) × 12° (longitude) within the area of 60° to 80° degrees north and south of the equator. A total of 853 data tiles cover the world in total, as shown in Figure 2.

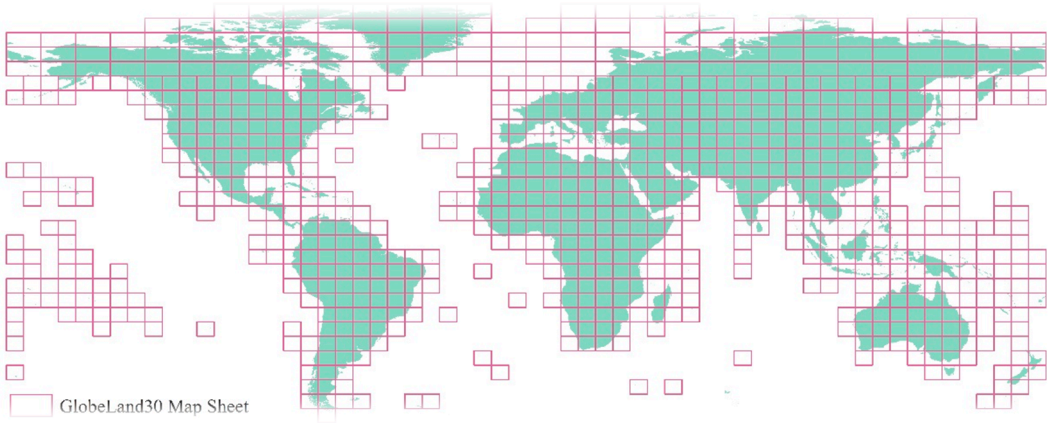


**Figure 2.** Data tiles of GlobeLand30.

### 2.2. Accuracy Analysis

The accuracy of GlobeLand30 had been evaluated by third-party researchers from more than ten countries for its all classes or one single class via sample-based validation or comparison with existing land cover products [28–30]. At the country/region level, a satisfactory overall accuracy was estimated as 82.4% for China [31], 80% for Italy [29], 77.90% for all of Iran [14], 80.1% for Nepal [32], and 89.7% for Kyiv Oblast, Ukraine [33]. Yang et al. [31] evaluated the accuracy of seven land cover products over China, namely, International Geosphere-Biosphere Program Data and Information System's land cover dataset (IGBP DISCover), The University of Maryland land cover dataset (UMD), Global Land Cover 2000 dataset (GLC2000) from the European Commission's Joint Research Center (JRC), Moderate Resolution Imaging Spectroradiometer (MODIS) land cover products MOD12Q1 and MCD12Q1, Global Map–Global LC (GLCNMO) dataset from the International Steering Committee for Global Mapping, Climate Change Initiative land cover dataset (CCI-LC) from European Space Agency (ESA), and GlobeLand30; they found that GlobeLand30-2010 has the highest overall accuracy (82.4%). Arsanjani et al. [28] reported that GlobeLand30 has high agreements with CORINE (92.52%), Urban Atlas (85.43%), OpenStreetMap (74.24%), and ATKIS (85.23%) in Germany. Mozak [34] found that GlobeLand30 product overlap with a degree of 77% with GLC-Share product in Continental Portugal. However, a lower overall accuracy with 46% for the GlobeLand30-2010 was found in Central Asia, that is, Kazakhstan, Tajikistan, Turkmenistan, Uzbekistan, and Kyrgyzstan [35]. The major classification error might originate from the confusion between bare land and grassland [33,36] because of discrepancies of land cover type definitions. Table 2 lists the accuracy assessment results for GlobeLand30 in the literature.

Accuracy assessment has also been conducted for certain single land cover types of GlobeLand30. Manakos et al. [30] found that land surface water of GlobeLand30 overlaps 91.9% of the reference data in Thessaly, Greece, whereas the coarser-resolution products are restricted to lower accuracies. Lu et al. [37] compared cropland class of five global cropland datasets in circa 2010 of China, including GlobeLand30, Finer Resolution Observation and Monitoring GLC dataset (FROM-GLC), GlobCover, MODIS Collection 5, and MODIS Cropland. The results showed that the overall accuracy of cropland of GlobeLand30 is 79.61%, which is highest in the five products. Chen et al. [38] evaluated the accuracy of cropland for GlobeLand30, MODIS land cover product, GlobCover2009, and FROM-GLC in Shaanxi, China, and the overall accuracy for GlobeLand30 is 80.63%.

**Table 2.** Examples of accuracy evaluation of GlobeLand30 from published articles.

| Scale | Region | Classes for Evaluation | Accuracy | References |
|---|---|---|---|---|
| Sub-continental | Central Asia | 10 classes | 46.0% | Sun et al., 2016 [35] |
| | East Africa | Cropland | 83.1% | Jacobson, 2015 [39] |
| National | China | 10 classes | 82.4% | Yang et al., 2017 [31] |
| | Iran | 10 classes | 77.9% | Arsanjani et al., 2016b [28] |
| | Italy | 10 classes | 80.0% | Brovelli et al., 2015 [29] |
| | Nepal | 10 classes | 80.1% | Cao et al., 2016 [32] |
| | Portugal | 10 classes | 77.0% | Mozak, 2016 [34] |
| | China | Cropland | 79.6% | Lu et al., 2016 [40] |
| | China | Forest | 87.0% | Wang et al., 2015 [41] |
| Regional | Siberia, Russia | 10 classes | 86.9% | Zhang et al., 2015a [42] |
| | Kyiv Oblast, Ukraine | 10 classes | 89.7% | Kussul et al., 2015 [33] |
| | Henan Province, China | 10 classes | 81.5% | Ma et al., 2016 [43] |
| | Thessaly, Greece | Water | 91.9% | Manakos et al., 2015 [30] |
| | Shaanxi province, China | Cropland | 80.6% | Chen et al., 2017 [44] |

## 3. User Analysis

### *3.1. Geographical Distribution*

GlobeLand30 has been downloaded by more than 7000 users since its release for open access in 2014. Over 5000 users are registered in the GlobeLand30 data platform [25]. The other users downloaded data from Global Change Research Data Publishing and Repository [45]. The downloading frequency of GlobeLand30 data tiles is shown in Figure 3, where the darker color represents the higher downloading frequency, and the areas with slashes represent the countries with registered users. Higher downloading is concentrated in developing countries (such as those in Africa and Asia), thereby accounting for over 72%. Kenya, Tanzania, and Uganda have the highest downloading frequencies in Africa. The areas with the highest frequencies in Asia are in South and South East Asia, especially in India, Pakistan, Nepal, Myanmar, Thailand, and Laos. One reason might be the limited high quality and open access land cover datasets in these areas. The other reason is that some of these areas are of interest or are hot spots. For examples, GlobeLand30 datasets have been used to land cover studies, and disaster mapping and assessment in Nepal and Myanmar [15,46,47].

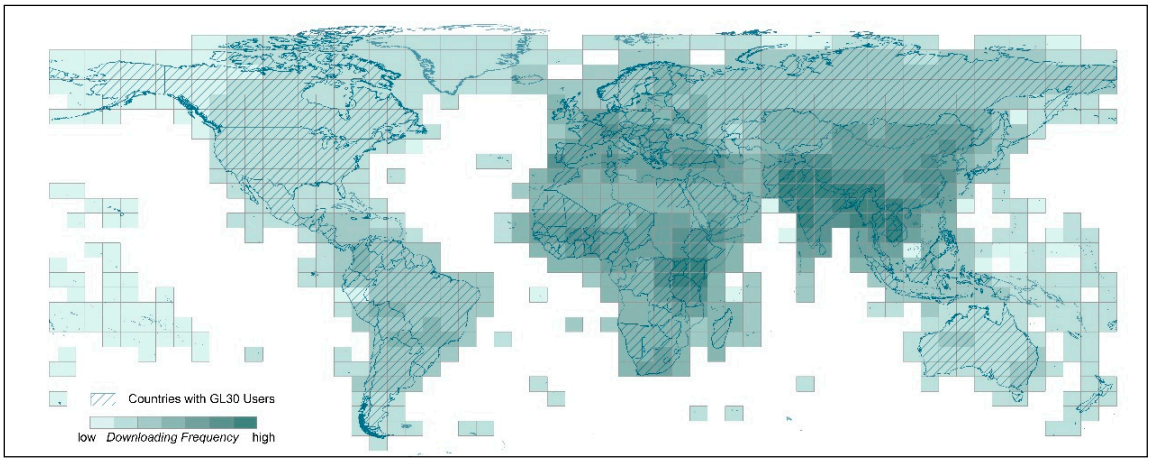


**Figure 3.** User's geographical distribution and download frequency of GlobeLand30.

As of April 2017, users from over 120 countries have downloaded GlobeLand30. The top ten countries with the most user numbers are China, the U.S., India, the UK, Germany, Canada, France, Brazil, The Netherlands, and Russia. Most of the users come from universities, research institutions,

and government departments. More specifically, more than half of users are from the laboratories of universities, such as Harvard University, Princeton University, the University of Heidelberg, Peking University, and so on. One in every four users of GlobeLand30 are from scientific research institutions, such as the Joint Research Centre of the European Commission, the Institute for Global Environmental Strategies, the Helmholtz-Centre Potsdam-German Research Centre for Geosciences, and so on. Many UN agencies and non-governmental organizations are also users of GlobeLand30. For example, the UN Field Operation Department has used GlobeLand30 to assist the analysis and development of peacekeeping action plans in 18 countries. The UN Economic and Social Commission for Asia and the Pacific used GlobeLand30 to support drought management and land degradation. The UN Environment Programme's World Conservation Monitoring Centre (UNEP-WCMC) used GlobeLand30 for the land cover analysis for the protected areas worldwide.

### *3.2. Application Fields*

GlobeLand30 data has been widely used in a number of Social Benefits Areas (SBAs), including climate change adaptation, biodiversity and ecosystem sustainability, disaster resilience, energy and mineral resources management, food security and sustainable agriculture, infrastructure and transportation management, public health surveillance, sustainable urban development, water resources management, and so on. Table 3 summarizes its applications in these SBAs based on the user registration information. The biodiversity and ecosystem is the largest application area and comprises over 26% in all research areas. The second largest application area of GlobeLand30 is sustainable urban development, accounting for nearly 16% of all applications. The applications in disaster resilience, food security and sustainable, and water resources management have proportions of over 10%.

**Table 3.** Major application fields of GlobeLand30.

| Research Fields | Proportion of Each Field | University | Institute | Government | NGO | UN | Other |
|---|---|---|---|---|---|---|---|
| **Climate Change** | **7.51%** | *38.62%* | *31.29%* | *7.32%* | *9.32%* | *3.06%* | *10.39%* |
| **Biodiversity and Ecosystem** | **26.94%** | *48.85%* | *32.26%* | *0.59%* | *3.19%* | *1.15%* | *13.96%* |
| **Disaster Resilience** | **13.69%** | *73.78%* | *10.30%* | *9.72%* | *1.68%* | *2.26%* | *2.26%* |
| **Energy and Mineral Resources Management** | **5.33%** | *29.46%* | *29.46%* | *20.64%* | *4.32%* | *0.00%* | *16.14%* |
| **Food Security and Sustainable Agriculture** | **10.09%** | *48.86%* | *16.25%* | *3.87%* | *12.39%* | *6.24%* | *12.39%* |
| **Infrastructure and Transportation Management** | **3.84%** | *48.96%* | *26.56%* | *2.08%* | *12.24%* | *0.00%* | *10.16%* |
| **Public Health Surveillance** | **4.06%** | *40.39%* | *38.67%* | *3.94%* | *5.67%* | *5.67%* | *5.67%* |
| **Sustainable Urban Development** | **15.98%** | *64.21%* | *19.59%* | *6.38%* | *2.44%* | *1.00%* | *6.38%* |
| **Water Resources Management** | **12.53%** | *59.38%* | *19.39%* | *7.50%* | *1.84%* | *0.64%* | *11.25%* |
| **Proportion of each organization** | **100.00% (Sum)** | **53.88%** | **23.81%** | **5.72%** | **4.62%** | **1.96%** | **10.02%** |

Note: The italic figures mean the relative proportion of each organization in this research filed, and the sum of each line is 100%.

The number of users from universities and institutes has exceeded 75% of all users. Roughly 60% of applications of GlobeLand30 in laboratories of universities are found in biodiversity and ecosystem, energy and mineral resources management, and sustainable urban development. One of the reasons for this use is the ability of the 30 m land cover dataset to represent ecologically-relevant features at multiple spatial scales, thereby making it a powerful tool for studying ecological environment distributions [48]. Beijing Normal University used GlobeLand30 to analyze the impacts of land cover change on ecosystem service values over a 10-year period and summarized that the negative impacts of urban expansion on ecosystem services can be offset by positive changes to natural landscapes,

because a change in ecosystem service value depends on the interaction of changes of various land cover types over time [49]. Given that reliable information on cities' changes at a global scale will become increasingly important with climbing urban populations [50], Peking University investigated the spatial-temporal variation of habitat quality patterns of Beijing-Tianjin-Hebei area based on the analysis of GlobeLand30 from 2000 to 2010 [51].

Many research institutions have used GlobeLand30 for biodiversity and ecosystem, sustainable urban development, water resource management, and climate change. For instance, the National Geomatics Center of China analyzed the distribution of built-up areas, change rate, and increased proportion on a global scale by GlobeLand30 [52]. The National Climate Center of China used GlobeLand30 as a basic input parameter in the Beijing Climate Center Climate System Model (BCC_CSM) to assess the effects of land cover dataset on land surface and climate simulations [53].

Government departments mainly used GlobeLand30 for analysis and research in disaster resilience, energy and mineral resources management, and sustainable urban development. Most applications in Non-Governmental Organizations (NGOs) and the UN are food security and sustainable agriculture, biodiversity and ecosystem sustainability, and public health surveillance. Timely and accurate geographic information on the global cropland extent is critical for applications in the fields of food security and agricultural monitoring. Thus, Waldner et al. [54] advocated for a shared definition of cropland, as well as validation datasets that are relevant for the agricultural class by studying different land cover data.

## 4. Application Analysis

GlobeLand30 provides useful information with higher spatial resolution for different research fields. These include quantifying land use for each watershed in Panamanian drainage basins [55]; identifying types of sampling sites based on the hydrology and land-use characteristics to monitor contaminants in river sediments [46–57], discriminating fire types from MODIS active fire products, such as forest fire, grassland fire, agricultural burning and so on [58]; assessing flooded arable land of a major flood in Myanmar [46]; selecting eddy-covariance flux towers with relatively homogenous land cover in the light use efficiency models to simulate GPP [59]; analyzing habitat of bats in Lao PDR and Cambodia [60–62]; and providing validation sources to evaluate the classification performance of the water body extraction from MODIS eight-day products [62]. In particular, GlobeLand30 data has been used to derive useful information about the status and change of land cover, to examine their causes and consequence analysis, and to explore future development scenarios.

### *4.1. Status and Change Analysis*

The status and change of land cover at global, regional or local scales has been studied using GlobeLand30 and with spatial statistical analysis approaches. At the global scale, Cao et al. [63] used GlobeLand30's water layer data to analyze the distribution of global open water and change from 2000 to 2010. Two indicators, namely, water body percentage and the coefficient of spatial variation, were calculated to reflect the characteristics of spatial distribution pattern and dynamic change for global open water resources. Results show that the total area of land surface water is roughly 3.68 million $km^2$ (2010), which occupies 2.73% of the Earth's land surface. Similarly, Chen et al. [52] calculated global artificial surface areas at country and continental scales, and analyzed its change between 2000 and 2010. The result shows that the total area of the global built-up areas is 1.1875 million $km^2$ in 2010, covering 0.88% of the total area of the global land surface; the area of global built-up areas increased to 57,400 $km^2$ with the variation rate of 5.08% from 2000 to 2010. China and the United States are the top two countries with the largest increased built-up areas, which account for roughly 50% of that of the global total. In addition, 50.26% of the total increased built-up areas comes from arable land.

Areas, landscape indexes, and conversion matrix were used to analyze the status and change of land covers at the country/regional scale. Putrenko [64] calculated the Shannon index from GlobeLand30 to reveal the diversity of land cover types in administrative regions of Ukraine.

Yang et al. [65] derived the conversion matrix, change rate, and landscape indices from GlobeLand30 to analyze land cover change, especially the loss of cultivated land for the Bohai Rim, China between 2000 and 2010. Results indicate that cultivated land obviously reduced and was mainly converted to artificial surfaces, grasslands, water, and forests in this region, and the fragmentation of cultivated land increased. Cao et al. [32] calculated and compared the areas of forest, shrub, grassland, wetland, cropland, artificial surface, bare land and ice/snow in GlobeLand30 and a new NepalCover-2010. The landscape indices were used to demonstrate the spatial pattern of land cover types.

At the local scale, landscape metrics were derived from GlobeLand30 to quantify the landscape structure and to reveal the spatial details of land covers. Six landscape metrics are calculated for 25 cities in Yangtze River Delta, China from the artificial surface class of GlobeLand30, including total urban area (CA), number of urban patches (NP), largest patch index (LPI), mean perimeter-area ratio (PARA MN), mean Euclidean nearest neighbor distance (ENN MN), and traffic coupling factor (CF) with a spatial pattern analysis program FRAGSTATS 4.2 [66,67]. These metrics were used to analyze the relationship between urban forms and air quality. Chen, Zhu et al. [68] derived seven landscapes from GlobeLand30 in Nanjing, China for each of the nine PM2.5 stations with radii of 0.5, 1.0, 2.0, 3.0, 4.0, 5.0, and 6.0 km and applied FRAGSTATS to compute the metrics, such as green cover, forest cover, grassland cover, and edge length. These metrics were then used to quantify the spatiotemporal change of PM2.5 concentration and its empirical relationship with vegetation and landscape structure.

### *4.2. Cause and Consequence Analysis*

Global urban areas, croplands, and plantations have enlarged dramatically in recent years, and have seriously impacted resources sustainability, food security, ecological diversity, and climate change [2]. For example, clearing of tropical forests for cultivation or grazing is responsible for 12–26% of the total emissions of carbon dioxide to the atmosphere [69,70], and land use changes can significantly modify regional and global climate [3,71]. Furthermore, 20–30% of the total available surface water on the planet is withdrawn for irrigation [72], and nitrogen fixation via fertilizer production and crop cultivation currently equals, or even exceeds, natural biotic fixation [73,74]. GlobaLand30 offers a detailed portrait of such land covers, and enables researchers to understand how the current pattern forms, and the impact of GLC on the environment. Domain-specific data and methodologies need to be included in the cause and consequence analysis.

One of the examples is the cause and consequence analysis of human settlement expansion at the global scale [15]. Several indicators were derived from the artificial surface layer of GlobeLand30, such as the artificial surface area per capita, population per unit area of artificial surface, gross domestic product (GDP) per unit area of artificial surface, relative population increase to artificial surface increase, and relative GDP increase to artificial surface increase. These indicators were used to reveal the artificial surface use efficiencies pattern, relationship with population and GDP, and the change during 2000–2010 at the country level. Results show that the use efficiency of artificial surfaces has distinct regional discrepancies (Figure 4), in which Canada and the United States are categorized as having abundant resources, but low land use efficiency, and South Korea, Japan, and Switzerland are characterized by limited resources but high land use efficiency. Yu et al. [16] calculated the urban expansion intensity index (UEII) based on the ratio of the region's newly-appeared urban land areas to the total area within each ring from the city center. By plotting the UEII by distance to city center, a lognormal curve model was used to fit the curve. The fitting parameters were further used to calculate shape indexes of the curves, and their relationship among Chinese cities was analyzed.

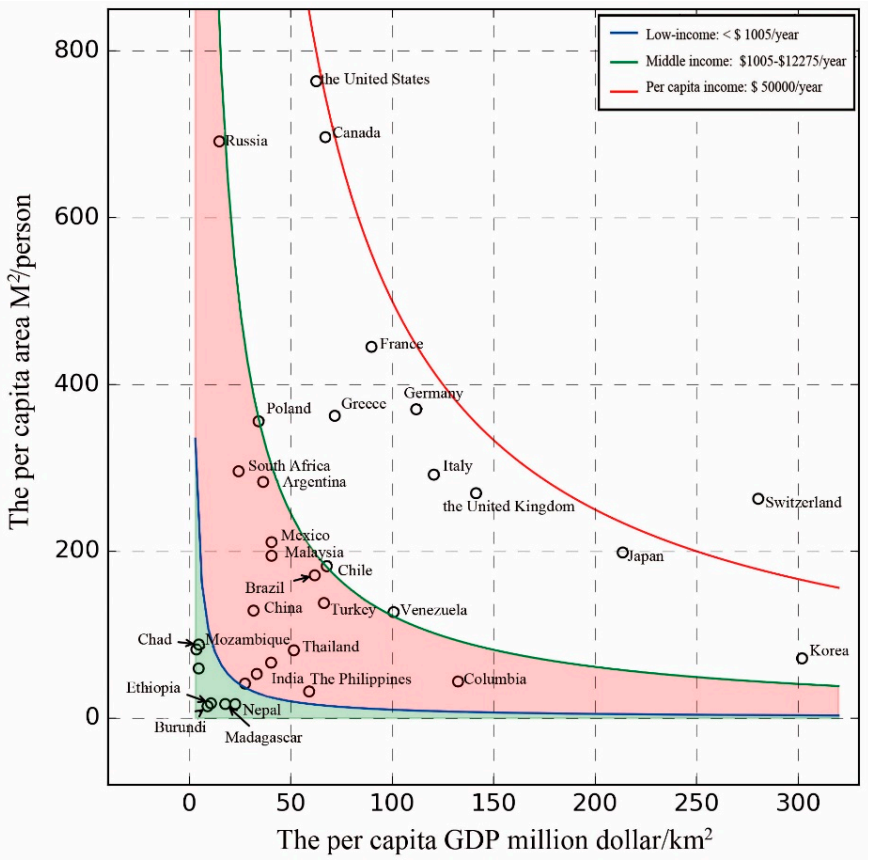


**Figure 4.** Artificial land use efficiencies at country level (adapted from Li et al. 2016 [15]).

GlobeLand30 was also used to reveal the impact of GLC on regional biogeochemical circle and ecosystem. Lu, Jiang et al. [40] extracted land-use transitions in China from GlobeLand30 2000 and 2010 products, including transitions among forest, grassland, cropland, and artificial surface, and then evaluated the effects of land cover change on N deposition based on the estimated N deposition data from $NO_2$ column remote sensing data (Global Ozone Monitoring Experiment, GOME, and Ozone Monitoring Instrument, OMI) and the GlobeLand30 dataset. The coupling effects of N deposition and land cover change on carbon budgets in China was also assessed based on a terrestrial ecosystem process-based model IBIS (Integrated Biosphere Simulator). Ende [75] used the land use regression model to simulate air pollution by using land use data from the Corine land cover dataset or the alternative GlobeLand30 in Bangkok and Mexico City. The response variable in the regression model is air pollution, and the explanatory variables are land use, traffic density, and topography. Kim et al. [76] used GlobeLand30 to calculate carbon budget in North Korea, and analyzed the future carbon budget in scenarios of climate change. Wang and Zhao [77] evaluated the ecological environment quality in Shaanxi, China, by calculating a synthetical ecological index from GlobaLand30-based biological richness index and vegetation coverage index at the 250 m level. Kühling et al. [78] calculated proportion of grassland in total area of district/province in the Western Siberian grain belt, and then calculated the grassland intensity for every year (1996–2013) as the product of grazing livestock density, the proportion of grassland per province/district area, and the proportion of grazing livestock units kept by households. Ge et al. [79] computed the ratio of the sum of the area of rivers, lakes, and reservoirs to the total area, which is an index to describe the fundamental ecological conditions of malaria transmission. Ding et al. [80] computed the percentage of seven land-use types, namely, forest, farmland, urban, grass, shrub, wetland, and water within each watershed of the upper Mekong River Basin, China to analyze the responses of functional traits and diversity of stream macroinvertebrates to environmental and spatial factors.

### 4.3. Coupling Analysis with Earth System Models

Models have proven to be an important tool, both to conceptualize and test human understanding of the role of different drivers in land use and land cover change and to explore scenarios of possible future developments [81,82]. In recent years, study on climate coupling models between the dynamic mechanism of land cover and environmental change has elicited considerable research interest in climate change, such as urban expansion and climate change. At present, the direct and indirect effects of land cover data on climate and climate change are receiving increasing attention. Models that use land cover information are mainly the climate model, urban change models, and environment model. For instance, urban expansion has been simulated by coupling one "bottom-up" cellular automata (CA)-based model and one "top-down" system dynamics (SD)-based model [83]. Here, we summarized some Earth system models that incorporate GlobeLand30 land cover information to simulate climate, hydrological cycle, and land surface fluxes.

GlobeLand30 dataset was used in the Beijing Climate Center Climate System Model (BCC_CSM) to assess the influences of land cover dataset on land surface and climate simulations. Land cover is one of the most basic input elements of land surface and climate models [52]. GlobeLand30 data was merged with other satellite remote sensing datasets to regenerate the plant function types (PFT) fitted for the BCC_CSM. The area-weighted up-scaling approach was used to aggregate the 30 m-resolution GlobeLand30 data onto the coarser model grids and derive PFT, as well as percentage information. Results show that with the new LC data products, several model biases between simulations and observations in the BCC climate model with original LC datasets were effectively reduced, including the positive bias of precipitation in the mid-high latitude of the northern hemisphere and the negative bias in the Amazon, as well as the negative bias of air temperature in parts of the southern hemisphere. Therefore, the GlobeLand30 data are considered suitable for use in the BCC_CSM component models and can improve the performance of the land and atmosphere simulations.

GlobeLand30 was also used as an input data in the Soil and Water Assessment Tool (SWAT) to model water vulnerability in the Yangtze River Basin, China [35]. Madhusoodhanan et al. [84] assessed the uncertainties of seven GLC datasets and their propagation into the simulation of land surface fluxes (LSFs) in India by using a macro-scale land surface model. The GLC datasets, including UMD, IGBP DISCover, GLC2000, MODIS, GlobeCover, CCI-LC and GlobeLand30, were aggregated to 0.25 degrees and then input into the variable infiltration capacity (VIC) model to simulate LSFs. The results were validated by observed stream flow and MODIS-derived global evapotranspiration data. The results indicated that GlobeLand30 with the least difference in crop fraction has the least bias. These studies showed that finer-resolution GLC land cover dataset can improve the accuracy of model simulation at the regional scale.

## 5. Discussion and Outlook

Based on the data downloading records and published literature, this paper has reviewed the analysis and applications of GlobeLand30 since its release in 2014. GlobeLand30 has been recognized by international scientific and user communities, such as being the world's first wall-to-wall 30 m GLC data product [85], "a milestone achievement in the Earth observation and open geo-information access." [13]. However, GlobeLand30is far from satisfying all user requirements, and the system has considerable room for improvement, such as more comprehensive validation, continuous updating, and more value-added applications.

### 5.1. Comprehensive Validation

The quality or accuracy assessment is an integral part of GLC mapping and applications. Third-party researchers or users have analyzed the quality of GlobeLand30 via sample-based validation or comparison with existing land cover or other datasets. An average accuracy of 80% for all classes or one single class was given by most published papers or documents [14,29,37,86]. Diogo and

Koomen [87] reported that the quality of GlobeLand30 was at a similar level to CORINE data. Grekousis et al. [7] summarized the reported accuracy of 23 global and 41 regional LC products, in which GlobeLand30 products have relatively high overall accuracy (78.6% and 80.3% for 2000 and 2010, respectively) compared with GLC2000 (68.6%), GlobCover2005 (73.1%), GlobeCover2009 (67.5%), UMD (65.0%), MODIS (71.6%), GLCNMO V2 (77.9%), FROM-GLC (63.69%), GeoWiki hybrid 1 (87.9%) and so on. GlobeLand30 is then recommended for diverse applications, including climate change studies, land change research, and ecosystem analysis [28,88]. In particular, GlobeLand30 is considered a useful product for developing countries or regions in which good land cover maps are difficult to find [14,89].

However, these accuracy assessments were conducted either within 10% map sheets selected from a global scale [24] or in some individual countries [14,86]. Areas remain in which the uncertainty of GlobeLand30 must be validated and documented. An international validation was initiated by GEO Global Land Cover Community Activity (GEO CA-01) in 2016 with three tasks to promote more comprehensive validation of GlobeLand30 and other finer-resolution GLC datasets. First, a technical specification was formulated to describe the appropriate approaches and procedures for sampling design, response, and analysis protocols at 30 m resolution and global scales. A landscape shape index (LSI)-based sampling approach was developed to consider the high spatial heterogeneity of land cover in large areas [37]. Two web-based validation tools were developed to facilitate online and collaborative validation processes. One tool is GLCVal [90] developed by the National Geomatic Center of China, and the other is LACO-Wiki [91] developed by the International Institute for Applied Systems Analysis (IIASA). Approximately 40 countries have joined this GEO-led activity and completed the validation for their own territory. More countries are expected to join the validation of GlobeLand30 and other finer-resolution GLC datasets in the near future.

### *5.2. Continuous Updating*

GlobeLand30 has users from more than 120 countries on five continents. As such, GlobeLand30 has been identified as a fundamental geospatial dataset by a number of international organizations, such as UN Committee of Experts on Global Geospatial Information Management (UN-GGIM) [89], UNEP [12], and Global Observation for Forest Cover and Land Dynamics (GOFC/GOLD) [90]. This has promoted data sharing in the field of geo-sciences and Earth observation, and stimulated the development of finer-resolution global land cover data products in the world [13,90]. However, a number of new requirements have been put forward by the users, such as more thematic classes, longer time series, and higher spatial resolution. For instance, GlobeLand30-2010 has ten major land cover classes, but more classes may be asked by certain applications, such as Ecosystem Accounting [91] and integrated biodiversity monitoring [12]. A total of 15 classes will be offered by the 2015 version of Gloebland30 which is under development. Since one single GLC dataset will never be perfectly suited for all applications either in terms of the legend or the accuracy, developing a new philosophy for generating land cover products by designing an operational system that can meet varied user requirements is important [92].

Time-series land cover data products are essential for understanding land cover dynamics, identifying its trends, as well as assessing social, economic, and environmental impacts. Although GlobeLand30 has only two base-line years (2000/2010), several other GLC maps with more epoch series have been developed. One is the CCI-LC product that covers three-epoch series (2008–2012, 2003–2007, 1998–2002) [87,93]. The resolution of CCI-LC data product is relatively coarse (300 m) and may not reveal certain land cover and its changes. The other time-series GLC map is the annual global tree cover maps that are produced by Hansen et al. (2013) with a high temporal resolution (annual forest cover change from 2000 to 2012), but is limited only to the percent tree cover/tree cover change. The development and provision of time-series 30 m and full class GLC maps is a significant challenge. This will be implemented by combining the mainstream change detection-based approach with the rapidly-increasing crowdsourced information [94,95].

Specific tools and systems need to be developed to support "faster" and operational GLC data product generation and updating, such as discovering useful alternative and ancillary information from the deep web [96,97], service relation-driven detection [98,99], trust of volunteered data [100], integration of crowdsourcing information [101]. At present, GEO is examining the possibility to develop a so-called "Data Cube" with the flexible classification concept, which will facilitate the on-demand extraction of land cover classes with deep learning and other data mining algorithms [92]. Another direction is to provide a web-based tool in which can design their own legends online and generate the desired land cover product [102,103].

### *5.3. Monitoring Progress towards Sustainable Development Goals (SDGs)*

The GlobeLand30 dataset has shown its potential in the status and change analysis, cause and consequence analysis, as well as the environmental parameterization of earth system models. The dataset has been listed as one of major GLC datasets to support monitoring progress towards the UN 2030 SDGs through its 230 indicators [88]. As a global and international data product, GlobeLand30 can be used first as a supplement or a potential alternative to national data when the reliable land cover data of one country is unavailable or lacks the capacity to generate them. Second, natural disasters, displaced populations, environmental change, water shortages, pandemics, and widespread malnutrition do not stop at national borders or the water's edge [104]. GlobeLand30 may have higher consistency across space, whereas the integration and harmonization of datasets from neighboring countries might be extremely difficult because of their differences in reference frames, spatial resolution, thematic types as well as periodicity. Third, global datasets can serve as a sound basis for preparing global reporting of certain SDG indicators and for visualizing or communicating their global status and trends to policy-makers and end users.

Methodological development and overall data availability are two challenges that face monitoring progress towards SDGs with GLC and other geospatial datasets. From the methodological point of view, analytical models, metrics, and tools need to be developed to compute or derive SDG indicators/indices from GLC or geospatial data. Sensitivity and uncertainty analysis need also be considered to test the efficacy and robustness of the computing approaches. As far as the overall data availability is concerned, a number of technical issues need to be solved to integrate GLC, statistical data and other geospatial data. For instance, disaggregation approaches will be developed and used for generating a dataset with a more refined thematic content by combining global data and ancillary data sources. Aggregation may be used to downscale high-resolution datasets into the desirable scale.

**Acknowledgments:** This work has been funded by Special Fund for Surveying, Mapping, and Geoinformation Scientific Research in the Public Welfare (grant no. 201512028), the National Science Foundation of China (project #41231172), and the 863 project of China (grant no. 2013AA122802).

**Author Contributions:** Jun Chen conceived and designed this review article; Xin Cao, Shu Peng and Huiru Ren contributed the literature and materials; Jun Chen and Xin Cao wrote and revised the paper.

**Conflicts of Interest:** The authors declare no conflict of interest.

## References

1. Lambin, E.F.; Helmut, J.G. (Eds.) *Land-Use and Land-Cover Change: Local Processes and Global Impacts*; Springer Science & Business Media: Berlin, Germany, 2008.
2. Foley, J.A.; DeFries, R.; Asner, G.P.; Barford, C.; Bonan, G.; Carpenter, S.R.; Chapin, F.S.; Coe, M.T.; Daily, G.C.; Gibbs, H.K.; et al. Global consequences of land use. *Science* **2005**, *309*, 570–574. [CrossRef] [PubMed]
3. Pielke, R.A. Land use and climate change. *Science* **2005**, *310*, 1625–1626. [CrossRef] [PubMed]
4. Sterling, S.; Ducharne, A. Comprehensive data set of global land cover change for land surface model applications. *Glob. Biogeochem. Cycles* **2008**, 22–23. [CrossRef]
5. Verburg, P.H.; Neuman, K.; Nol, L. Challenges in using land use and land cover data for global change studies. *Glob. Chan. Biol.* **2011**, *17*, 974–989. [CrossRef]

6. Reid, W.V.; Chen, D.; Goldfarb, L.; Hackmann, H.; Lee, Y.T.; Mokhele, K.; Ostrom, E.; Raivio, K.; Rockstrom, J.; Schellnhuber, H.J.; et al. Earth system science for global sustainability: Grand challenges. *Science* **2010**, *330*, 916–917. [CrossRef] [PubMed]
7. Grekousis, G.; Mountrakis, G.; Kavouras, M. An overview of 21 global and 43 regional land-cover mapping products. *Int. J. Remote Sens.* **2015**, *36*, 5309–5335. [CrossRef]
8. Verburg, P.H.; Kok, K.; Pontius, R.G., Jr.; Veldkamp, A. *Modeling Land-Use and Land-Cover Change*; Springer: Berlin/Heidelberg, Germany, 2006; pp. 117–135.
9. Verburg, P.H.; Crossman, N.; Ellis, E.C.; Heinimann, A.; Hostert, P.; Mertz, O.; Nagendra, H.; Sikor, T.; Erb, K. Land system science and sustainable development of the earth system: A global land project perspective. *Anthropocene* **2015**, *12*, 29–41. [CrossRef]
10. Zell, E.; Huff, A.K.; Carpenter, A.T.; Friedl, L.A. A user-driven approach to determining critical earth observation priorities for societal benefit. *IEEE J. Sel. Top. Appl. Earth Obs. Remote Sens.* **2012**, *5*, 1594–1602. [CrossRef]
11. Mora, B.; Tsendbazar, N.E.; Herold, M.; Arino, O. Global Land Cover Mapping: Current Status and Future Trends. In *Land Use and Land Cover Mapping in Europe*; Springer: Amsterdam, The Netherlands, 2014; pp. 11–30.
12. O'Connor, B.; Secades, C.; Penner, J.; Sonnenschein, R.; Skidmore, A.; Burgess, N.D.; Hutton, J.M. Earth observation as a tool for tracking progress towards the Aichi Biodiversity Targets. *Remote Sens. Ecol. Conserv.* **2015**, *1*, 19–28. [CrossRef]
13. Ban, Y.; Gong, P.; Giri, C. Global land cover mapping using Earth observation satellite data: Recent progresses and challenges. *ISPRS J. Photogramm. Remote Sens.* **2015**, *103*, 1–6. [CrossRef]
14. Arsanjani, J.J.; Tayyebi, A.; Vaz, E. GlobeLand30 as an alternative fine-scale global land cover map: Challenges, possibilities, and implications for developing countries. *Habitat Int.* **2016**, *55*, 25–31. [CrossRef]
15. Li, R.; Kuang, W.H.; Chen, J.; Chen, L.; Liao, A.; Peng, S.; Guang, Z. Spatio-temporal pattern analysis of artificial surface use efficiency based on GlobeLand30. *Sci. Sin. Terrae* **2016**, *46*, 1436–1445. (In Chinese)
16. Yu, X.; Zhang, B.Q.; Li, Q.; Chen, J. A method characterizing urban expansion based on land cover map at 30 m resolution. *Sci. China Earth Sci.* **2016**, *59*, 1738–1744. [CrossRef]
17. Brown, G. The relationship between social values for ecosystem services and global land cover: An empirical analysis. *Ecosyst. Serv.* **2013**, *5*, 58–68. [CrossRef]
18. Nagendra, H.; Reyers, B.; Lavorel, S. Impacts of land change on biodiversity: Making the link to ecosystem services. *Curr. Opin. Environ. Sustain.* **2013**, *5*, 503–508. [CrossRef]
19. Raymond, P.A.; Hartmann, J.; Lauerwald, R.; Sobek, S.; McDonald, C.; Hoover, M.; Butman, D.; Striegl, R.; Mayorga, E.; Humborg, C.; et al. Global carbon dioxide emissions from inland waters. *Nature* **2013**, *503*, 355–359. [CrossRef] [PubMed]
20. Sterling, S.M.; Ducharne, A.; Polcher, J. The impact of global land-cover change on the terrestrial water cycle. *Nat. Clim. Chang.* **2013**, *3*, 385–388. [CrossRef]
21. Giri, C.; Pengra, B.; Long, J.; Loveland, T.R. Next generation of global land cover characterization, mapping, and monitoring. *Int. J. Appl. Earth Obs. Geoinf.* **2013**, *25*, 30–37. [CrossRef]
22. Scoones, I.; Hall, R.; Borras Jr, S.M.; White, B.; Wolford, W. The politics of evidence: Methodologies for understanding the global land rush. *J. Peasant Stud.* **2013**, *40*, 469–483. [CrossRef]
23. Hansen, M.C.; Potapov, P.V.; Moore, R.; Hancher, M.; Turubanova, S.A.; Tyukavina, A.; Thau, D.; Stehman, S.V.; Goetz, S.J.; Loveland, T.R.; et al. High-resolution global maps of 21st-century forest cover change. *Science* **2013**, *342*, 851–853. [CrossRef] [PubMed]
24. Chen, J.; Chen, J.; Liao, A.; Cao, X.; Chen, L.; Chen, X.; He, C.; Han, G.; Peng, S.; Lu, M.; et al. Global land cover mapping at 30 m resolution: A POK-based operational approach. *ISPRS J. Photogramm. Remote Sens.* **2015**, *103*, 7–27. [CrossRef]
25. GlobeLand30 Data Platform. Available online: http://www.globallandcover.com (accessed on 21 July 2017).
26. Chen, J.; Chen, J.; Liao, A.; Cao, X.; Chen, L.; Chen, X.; Peng, S.; Han, G.; Zhang, H.; He, C.; et al. Concepts and key techniques for 30-m global land cover mapping. *Acta Geodaetica Cartographica Sin.* **2014**, *43*, 551–557. (In Chinese with English abstract)
27. Chen, J.; Ban, Y.; Li, S. China: Open access to Earth land-cover map. *Nature* **2014**, *514*, 434.
28. Arsanjani, J.J.; See, L.; Tayyebi, A. Assessing the suitability of GlobeLand30 for mapping land cover in Germany. *Int. J. Earth* **2016**, *9*, 873–891. [CrossRef]

29. Brovelli, M.A.; Molinari, M.E.; Hussein, E.; Chen, J.; Li, J. The first comprehensive accuracy assessment of GlobeLand30 at a national level: Methodology and results. *Remote Sens.* **2015**, *7*, 4191–4212. [CrossRef]
30. Manakos, I.; Chatzopoulos-Vouzoglanis, K.; Petrou, Z.I.; Filchev, L.; Apostolakis, A. Globalland30 mapping capacity of land surface water in Thessaly, Greece. *Land* **2015**, *4*, 1–18. [CrossRef]
31. Yang, Y.; Xiao, P.; Feng, X.; Li, H. Accuracy assessment of seven global land cover datasets over China. *ISPRS J. Photogramm. Remote Sens.* **2017**, *125*, 156–173. [CrossRef]
32. Cao, X.; Li, A.; Lei, G.; Lei, G.; Tan, J.; Zhang, Z.; Yan, D.; Xie, H.; Zhang, S.; Yang, Y.; et al. Land cover mapping and spatial pattern analysis with remote sensing in Nepal. *J. Geoinform. Sci.* **2016**, *18*, 1384–1398. (In Chinese with English abstract)
33. Kussul, N.; Shelestov, A.; Basarab, R.; Skakun, S.; Kussul, O.; Lavreniuk, M. Geospatial Intelligence and Data Fusion Techniques for Sustainable Development Problems. ICTERI, 2015. Available online: http://ceur-ws.org/Vol-1356/paper_48.pdf (accessed on 21 July 2017).
34. Mozak, S. Comparing Global Land Cover Datasets through the Eagle Matrix Land Cover Components for Continental Portugal. Master's Thesis, Nova Information Management School, Lisbon, Portugal, 26 February 2016. Available online: https://run.unl.pt/handle/10362/17653 (accessed on 21 July 2017).
35. Sun, B.; Chen, X.; Zhou, Q. Uncertainty Assessment of GLOBELAND30 Land Cover Data Set over Central Asia. *ISPRS-Int. Arch. Photogramm. Remote Sens. Spatial Inf. Sci.* **2016**, *XLI-B8*, 1313–1317. [CrossRef]
36. Sun, F.; Kuang, W.; Xiang, W.; Che, Y. Mapping water vulnerability of the Yangtze River Basin: 1994–2013. *Environ. Manag.* **2016**, *58*, 857–872. [CrossRef] [PubMed]
37. Lu, M.; Wu, W.; Zhang, L.; Liao, A.; Peng, S.; Tang, H. A comparative analysis of five global cropland datasets in China. *Sci. China Earth Sci.* **2016**, *59*, 2307–2317. [CrossRef]
38. Chen, F.; Chen, J.; Wu, H.; Hou, D.Y.; Zhang, W.W.; Zhang, J.; Zhou, X.G.; Chen, L.J. A landscape shape index-based sampling approach for land cover accuracy assessment. *Sci. China Earth Sci.* **2016**, *46*, 1413–1425. [CrossRef]
39. Jacobson, A.; Dhanota, J.; Godfrey, J.; Jacobson, H.; Rossman, Z.; Stanish, A.; Walker, H.; Riggio, J. A novel approach to mapping land conversion using Google Earth with an application to East Africa. *Environ. Model. Softw.* **2015**, *72*, 1–9. [CrossRef]
40. Lu, X.H.; Jiang, H.; Zhang, X.Y.; Jin, J.X. Relationship between nitrogen deposition and LUCC and its impact on terrestrial ecosystem carbon budgets in China. *Sci. China Earth Sci.* **2016**, *59*, 2285–2294. [CrossRef]
41. Wang, H.; Lv, Z.; Gu, L.; Wen, C. Observations of China's forest change (2000–2013) based on Global Forest Watch dataset. *Biodivers. Sci.* **2015**, *23*, 575–582. (In Chinese with English abstract) [CrossRef]
42. Zhang, Y.; Chen, J.; Chen, L.; Li, R.; Zhang, W.; Lu, N.; Liu, J. Characteristics of land cover change in Siberia based on GlobeLand30, 2000–2010. *Prog. Geogr.* **2015**, *34*, 1324–1333. (In Chinese with English abstract)
43. Ma, J.; Sun, Q.; Xiao, Q.; Wen, B. Accuracy assessment and comparative analysis of GlobeLand30 dataset in Henan province. *J. Geoinf. Sci.* **2016**, *18*, 1563–1572. (In Chinese with English abstract)
44. Chen, X.; Lin, Y.; Zhang, M.; Yu, L.; Li, H.; Bai, Y. Assessment of the cropland classifications in four global land cover datasets: A case study of Shaanxi Province, China. *J. Integr. Agric.* **2017**, *16*, 298–311. [CrossRef]
45. Global Change Research Data Publishing and Repository. Available online: www.geodoi.ac.cn (accessed on 21 July 2017).
46. Li, S.; Cui, Y.; Liu, M.; He, H.; Ravan, S. Integrating global open geo-information for major disaster assessment: Case study on Myanmar flood. *ISPRS Int. J. Geoinf.* **2017**, *6*, 201. [CrossRef]
47. Xue, W.; Gao, J.; Zhang, Y.; Liu, L.; Zhao, Z.; Paudel, B. Land Cover Status in the Koshi River Basin, Central Himalayas. *J. Resour. Ecol.* **2017**, *8*, 10–19. [CrossRef]
48. Xu, W.; Heys, B.; Fayrer-Hosken, R.; Presotto, A. Modeling the distribution of African Savanna elephants in Kruger National Park: An application of multi-scale GlobeLand30 data. *ISPRS-Int. Arch. Photogramm. Remote Sens. Spatial Inf. Sci.* **2016**, *XLI-B8*, 1327–1334. [CrossRef]
49. Zhang, Y.; Zhao, L.; Liu, J.; Liu, Y.; Li, C. The impact of land cover change on ecosystem service values in urban agglomerations along the coast of the Bohai Rim, China. *Sustainability* **2015**, *7*, 10365–10387. [CrossRef]
50. Frolking, S.; Milliman, T.; Seto, K.C.; Friedl, M.A. A global fingerprint of macro-scale changes in urban structure from 1999 to 2009. *Environ. Res. Lett.* **2013**, *8*, 24–40. [CrossRef]
51. Wu, J.; Cao, Q.; Shi, S.; Huang, X.; Lu, Z. Spatio-temporal variability of habitat quality in Beijing-Tianjin-Hebei Area based on land use change. *Chin. J. Appl. Ecol.* **2015**, *26*, 3457–3466. (In Chinese with English abstract)

52. Chen, J.; Chen, L.; Li, R.; Liao, A.; Peng, S.; Lu, N.; Zhang, Y. Spatial distribution and ten years change of global built-up areas derived from GlobeLand30. *Acta Geodaetica Vartographica Sin.* **2015**, *44*, 1181–1188. (In Chinese with English abstract)
53. Shi, X.L.; Nie, S.P.; Ju, W.M.; Yu, L. Climate effects of the GlobeLand30 land cover dataset on the Beijing Climate Center climate model simulations. *Sci. China Earth Sci.* **2016**, *59*, 1754–1764. [CrossRef]
54. Waldner, F.; Canto, G.S.; Defourny, P. Automated annual cropland mapping using knowledge-based temporal features. *ISPRS J. Photogramm. Remote Sens.* **2015**, *110*, 1–13. [CrossRef]
55. Gonzales, V.S.; Bierman, P.R.; Nichols, K.K.; Rood, D.H. Long-term erosion rates of Panamanian drainage basins determined using in situ 10Be. *Geomorphology* **2016**, *275*, 1–15. [CrossRef]
56. Xie, Y.; Wang, J.; Wu, Y.; Ren, C.; Song, C.; Yang, J.; Yu, H.; Giesy, J.P.; Zhang, X. Using in situ bacterial communities to monitor contaminants in river sediments. *Environ. Pollut.* **2016**, *212*, 348–357. [CrossRef] [PubMed]
57. Xie, Y.; Wang, J.; Yang, J.; Giesy, J.P.; Yu, H.; Zhang, X. Environmental DNA metabarcoding reveals primary chemical contaminants in freshwater sediments from different land-use types. *Chemosphere* **2017**, *172*, 201–209. [CrossRef] [PubMed]
58. Xie, H.; Du, L.; Liu, S.; Chen, L.; Gao, S.; Liu, S.; Pan, H.; Tong, X. Dynamic monitoring of agricultural fires in China from 2010 to 2014 using MODIS and GlobeLand30 data. *ISPRS Int. J. Geoinf.* **2016**, *5*, 172. [CrossRef]
59. Zhou, Y.; Wu, X.; Ju, W.; Chen, J.M.; Wang, S.; Wang, H.; Yuan, W.; Black, T.A.; Jassal, R.; Ibrom, A.; et al. Global parameterization and validation of a two-leaf light use efficiency model for predicting gross primary production across FLUXNET sites. *J. Geophys. Res. Biogeosci.* **2016**, *121*, 1045–1072. [CrossRef]
60. Lacroix, A.; Duong, V.; Hul, V.; San, S.; Davun, H.; Omaliss, K.; Chea, S.; Hassanin, A.; Theppangna, W.; Silithammavong, S.; et al. Diversity of bat astroviruses in Lao PDR and Cambodia. *Infect. Gen. Evol.* **2017**, *47*, 41–50. [CrossRef] [PubMed]
61. Lacroix, A.; Duong, V.; Hul, V.; San, S.; Davun, H.; Omaliss, K.; Chea, S.; Hassanin, A.; Theppangna, W.; Silithammavong, S.; et al. Genetic diversity of coronaviruses in bats in Lao PDR and Cambodia. *Infect. Gen. Evol.* **2017**, *48*, 10–18. [CrossRef] [PubMed]
62. Tong, X.; Pang, H.; Xie, H.; Xu, X.; Li, F.; Chen, L.; Luo, X.; Liu, S.; Chen, P.; Jin, Y. Estimating water volume variations in Lake Victoria over the past 22 years using multi-mission altimetry and remotely sensed images. *Remote Sens. Environ.* **2016**, *187*, 400–413. [CrossRef]
63. Cao, X.; Chen, J.; Chen, L.J.; Liao, A.P.; Sun, F.D.; Li, Y.; Li, L.; Lin, Z.H.; Pang, Z.G.; Chen, J.; et al. Preliminary analysis of spatiotemporal pattern of global land surface water. *Sci. China Earth Sci.* **2014**, *57*, 2330–2339. [CrossRef]
64. Putrenko, V. The spatial statistical generalization of information for regional land-use management in Ukraine. In Proceedings of the 1st ICA European Symposium on Cartography, EuroCarto 2015, Vienna, Austria, 10–12 November 2015.
65. Yang, Y.; Ma, X.; He, C. The loss process of cultivated land based on GlobeLand30: A case study of Bohai Rim. *China Land Sci.* **2016**, *30*, 72–79. (In Chinese with English abstract)
66. McGarigal, K.; Cushman, S.A.; Ene, E. FRAGSTATS v4: Spatial Pattern Analysis Program for Categorical and Continuous Maps. Computer software program produced by the authors at the University of Massachusetts, Amherst, 2012. Available online: http://www.umass.edu/landeco/research/fragstats/fragstats.html (accessed on 21 July 2017).
67. She, Q.; Peng, X.; Xu, Q.; Long, L.; Wei, N.; Liu, M.; Jia, W.; Zhou, T.; Han, J.; Xiang, W. Air quality and its response to satellite-derived urban form in the Yangtze River Delta, China. *Ecol. Indic.* **2017**, *75*, 297–306. [CrossRef]
68. Chen, J.; Zhu, L.; Fan, P.; Tian, L.; Lafortezza, R. Do green spaces affect the spatiotemporal changes of PM2.5 in Nanjing? *Ecol. Process.* **2016**, *5*, 7. [CrossRef] [PubMed]
69. DeFries, R.S.; Houghton, R.A.; Hansen, M.C.; Field, C.B.; Skole, D.; Townshend, J. Carbon emissions from tropical deforestation and regrowth based on satellite observations for the 1980s and 1990s. *Proc. Natl. Acad. Sci. USA* **2002**, *99*, 14256–14261. [CrossRef] [PubMed]
70. Houghton, R.A. Revised estimates of the annual net flux of carbon to the atmosphere from changes in land use and land management 1850–2000. *Tellus* **2003**, *55*, 378–390. [CrossRef]
71. Pitman, A.; Pielke, R., Sr.; Avissar, R.; Claussen, M.; Gash, J.; Dolman, H. The role of the land surface in weather and climate: Does the land surface matter. *Meso* **1999**, *2*, 20.

72. Cassman, K.G.; Wood, S. Cultivated systems. In *Ecosystems and Human Well-Being: Current State and Trend*; Balisacan, A., Gardiner, P., Eds.; Island Press: Washington, DC, USA, 2005; Volume 1, pp. 745–794.
73. Galloway, J.N.; Schlesinger, W.H.; Levy, H.; Michaels, A.; Schnoor, J.L. Nitrogen fixation: Anthropogenic enhancement-environmental response. *Glob. Biogeochem. Cycles* **1995**, *9*, 235–252. [CrossRef]
74. Smil, V. Nitrogen in crop production: An account of global flows. *Glob. Biogeochem. Cycles* **1999**, *13*, 647–662. [CrossRef]
75. Van den Ende, P. Modelling air Pollution and Personal Exposure in Bangkok and Mexico City Using a Land Use Regression Model, 2016. Available online: https://dspace.library.uu.nl/handle/1874/337072 (accessed on 21 July 2017).
76. Kim, D.; Lim, C.; Song, C.; Lee, W.; Piao, D.; Heo, S.; Jeon, S. Estimation of future carbon budget with climate change and reforestation scenario in North Korea. *Adv. Space Res.* **2016**, *58*, 1002–1016. [CrossRef]
77. Wang, C.; Zhao, H. The assessment of urban ecological environment in watershed scale. *Procedia Environ. Sci.* **2016**, *36*, 169–175. [CrossRef]
78. Kühling, I.; Broll, G.; Trautz, D. Spatio-temporal analysis of agricultural land-use intensity across the Western Siberian grain belt. *Sci. Total Environ.* **2016**, *544*, 271–280. [CrossRef] [PubMed]
79. Ge, Y.; Song, Y.; Wang, J.; Liu, W.; Ren, Z.; Peng, J.; Lu, B. Geographically weighted regression-based determinants of malaria incidences in northern China. *Trans. GIS* **2016**. [CrossRef]
80. Ding, N.; Yang, W.; Zhou, Y.; González-Bergonzoni, I.; Zhang, J.; Chen, K.; Vidal, N.; Jeppesen, E.; Liu, Z.; Wang, B. Different responses of functional traits and diversity of stream macroinvertebrates to environmental and spatial factors in the Xishuangbanna watershed of the upper Mekong River Basin, China. *Sci. Total Environ.* **2017**, *574*, 288–299. [CrossRef] [PubMed]
81. Parker, D.C.; Manson, S.M.; Janssen, M.A.; Hoffmann, M.J.; Deadman, P. Multiagent systems for the simulation of land-use and land-cover change: A review. *Ann. Assoc. Am. Geogr.* **2003**, *93*, 314–337. [CrossRef]
82. Matthews, R.; Gilbert, N.; Roach, A.; Polhill, J.G.; Gotts, N.M. Agent-based land-use models: A review of applications. *Landsc. Ecol.* **2007**, *22*, 1447–1459. [CrossRef]
83. He, C.; Okada, N.; Zhang, Q.; Shi, P.; Zhang, J. Modeling urban expansion scenarios by coupling cellular automata model and system dynamic model in Beijing, China. *Appl. Geogr.* **2006**, *26*, 323–345. [CrossRef]
84. Madhusoodhanan, C.G.; Sreeja, K.G.; Eldho, T.I. Assessment of uncertainties in global land cover products for hydro-climate modeling in India. *Water Resour. Res.* **2017**, *53*, 1713–1734. [CrossRef]
85. O'Connor, B.; Meng, H.; Burgess, N.; Hutton, J. *Towards a Multi-Decadal Global Land Cover Change Product—A Review for Biodiversity and Conservation*; United Nations Environment Programme: Nairobi, Kenya, 2014.
86. Manakos, I.; Karakizi, C.; Gkinis, I.; Karantzalos, K. Validation and inter-comparison of spaceborne derived global and continental land cover products for the Mediterranean region: The case of Thessaly. *Land* **2017**, *6*, 34. [CrossRef]
87. Diogo, V.; Koomen, E. *Land Cover and Land Use Indicators: Review of Available Data*; OECD Green Growth Papers, No. 2016/03; OECD Publishing: Paris, France, 2016.
88. Mora, B.; Romijn, E.; Herold, M. Monitoring progress towards Sustainable Development Goals—The role of land monitoring. In Proceedings of the 5th GEOSS Science and Technology Stakeholder Workshop—Linking the Sustainable Development Goals to Earth Observations, Models and Capacity Building, Berkeley, CA, USA, 9–10 December 2016.
89. UN-GGIM. Determination of Global Fundamental Geospatial Data Themes. Presented at the UN-GGIM Fifth Session, New York, NY, USA, 5–7 August 2015.
90. GLCVal. Available online: http://glcval.geo-compass.com (accessed on 21 July 2017).
91. LACO-Wiki. Available online: https://www.laco-wiki.net (accessed on 21 July 2017).
92. Peng, C.; Song, X.; Jiang, H.; Zhu, Q.; Chen, H.; Chen, J.M.; Gong, P.; Jie, C.; Xiang, W.; Yu, G.; et al. Towards a paradigm for open and free sharing of scientific data on global change science in China. *Ecosyst. Health Sustain.* **2016**, *2*, e01225. [CrossRef]
93. United Nations; European Commission; Food and Agriculture Organization; International Monetary Fund; OECD; World Bank. *System of Environmental-Economic Accounting 2012—Central Framework*; United Nations Statistics Division: New York, NY, USA, 2014.
94. Geller, G. Towards a New Philosophy for Generating Land Cover Products. In Proceedings of the ESA World Cover 2017, Rome, Italy, 14–16 March 2017.

95. Kirches, G.; Brockmann, C.; Boettcher, M.; Peters, M.; Bontemps, S.; Lamarche, C.; Schlerf, M.; Santoro, M.; Defourny, P. *CCI-LC Product User Guide*; UCL Geometrics: Brussels, Belgium, 2014.
96. Herold, M.; See, L.; Tsendbazar, N.E.; Fritz, S. Towards an Integrated Global Land Cover Monitoring and Mapping System. *Remote Sens.* **2016**, *8*, 1036. [CrossRef]
97. Chen, J.; Zhang, J.; Zhang, W.W.; Peng, S. Continuous updating and refinement of land cover data product. *J. Remote Sens.* **2016**, *20*, 991–1001. (In Chinese with English abstract) [CrossRef]
98. Hou, D.; Chen, J.; Wu, H. Discovering land cover web map services from the deep web with javascript invocation rules. *ISPRS Int. J. Geo-Inf.* **2016**, *5*, 105. [CrossRef]
99. Xing, H.; Chen, J.; Wu, H.; Zhang, J.; Li, S.; Liu, B. A service relation model for web-based land cover change detection. *ISPRS J. Photogram. Remote Sens.* **2017**. accepted.
100. Zhao, Y.J.; Zhou, X.G.; Li, G.Q.; Xing, H. A spatio-temporal VGI model considering trust-related information. *ISPRS Int. J. Geo-Inf.* **2016**, *5*, 10. [CrossRef]
101. Zhou, X.; Zeng, L.; Jiang, Y.; Zhou, K.; Zhao, Y. Dynamic Integrating OSM data to Borderland Database. *ISPRS Int. J. Geo-Inf.* **2015**, *4*, 1707–1728. [CrossRef]
102. Jung, M.; Henkel, K.; Herold, M.; Churkina, G. Exploiting synergies of global land cover products for carbon cycle modeling. *Remote Sens. Environ.* **2006**, *101*, 534–553. [CrossRef]
103. Xing, H.; Chen, J.; Wu, H.; Zhang, J.; Liu, B. An online land cover change detection system with web service composition. In Proceedings of the 4th IEEE International Workshop on Earth Observation and Remote Sensing Applications (EORSA), Bandung, Indonesia, 25–27 May 2016; pp. 275–279.
104. Suresh, S. Global challenges need global solutions. *Nature* **2012**, *490*, 337–338. [CrossRef] [PubMed]